

# Analysis and modelling of a swing check valve dynamic behaviour during blowdown experiments

P.Dumazert  
Framatome, Paris, France



## ABSTRACT

We exhibit in the present paper the phenomena occurring during the closure of a swing check valve and propose a modelling of its dynamic behaviour. Experimental and calculated results match quite well.

## 1 - INTRODUCTION

The aim of the swing check valve used in PWR lines is to prevent the complete emptying of the line and the capacity which bounds it when the flow is reversed. This occurs particularly when the line breaks. Unexpected large fluctuations may result from the stop of the reversed flow by the check valve. It appears essential to estimate as precisely as possible the intensity and the duration of the pressure surges to size the line in order to avoid a new break between the valve and the capacity.

Experiments on the test facility CLAUDIA (CEA Cadarache, FRANCE) have been conducted to analyze the closing behaviour of a swing check valve. This paper deals with these experiments. After applying ourself to point out the main phenomena, we expose a comparison between test data and calculation results. The study emphasizes the fluid-disc interaction.

## 2 - EXPERIMENTAL

In order to understand the phenomena met during the closure of a swing check valve, we choose and compare, among all the experiments, three tests.

### 2.1 Experimental apparatus and initial conditions

The figure 1 shows a sketch of the test line.

The expansion results from the burst of the membrane closing the line. The pressure transducers (points A and B, figure 1) allow us to get informations about the transient. The disc course is known by a displacement sensor.

More details on the experimental apparatus can be found in (1). The valve is shown in figure 2.

From one test set as reference (Test 1 : 3 MPa, 20 C, complete opening), two parameters have been explored :

- reduced opening (test 2 : 3 MPa, 20 C, mid-opening)
- temperature (test 3 : 3 MPa, 190 C, complete opening)

Figures 3 to 5 refer to the first test, figures 6 to 8 to the second and figures 9 and 10 to the third. Unfortunately, the displacement sensor failed during the third test.

## 2.2 Tests analysis

A detailed analysis and a comparison between the three experiments reveal four main phenomena in the dynamic behaviour of the valve.

- head loss effect
- wave effect
- induced flow rate effect
- disc bounce effect

### 2.2.1 Head loss effect

The head loss coefficient in reversed flow  $K$  is measured in permanent flow. Its curve versus  $\theta$  (1) has the following form : nearly constant if  $\theta$  is greater than fifteen degrees and decreasing in  $1/\theta^2$  if not. By comparing PA and PB for each test, it appears that the head loss effect become significant only during the last degrees of closure. This allows us to use the "permanent curve" of  $K$  in transient flow. As shown by figures 9 and 10, when no wave travels through the valve during the major part of the transient, the head loss effect is indeed the closing force.

### 2.2.2 Wave effect and induced flow rate effect (fig. 3,4,5 and 6,7,8)

The initial angular velocity of the disc is more important in the second test (2,7 rd/s) than in the first (0 rd/s). The initial expansion wave is obviously the same and a greater head loss coefficient in the second test cannot fully explain such a discrepancy.

In the second test, the initial valve contracted area is smaller than the pipe section. The expansion, partly reflected by the contracted area, is higher up-stream than down-stream of the valve and the disc is accelerated (figure 8). It pushes then in front of it some fluid toward the break. This added flow rate in the pipe induces the small pressure surge showing by the figure 6 around 6 ms. This surge reduces the velocity of the disc. When it vanishes, the disc will be accelerated again and a new pressure surge appears.

The valve disc motion is responsible for a fluid transfer whereby some fluid has to take the place left by the disc displacement. To cross the valve, the pipe flow rate splits into the flow rate beneath the disc and the induced flow rate.

During the braking, the induced flow rate is slowed down leading to a small compression wave which goes toward the capacity. It superimposes on the initial expansion the slope of which is smoother down-stream of the valve. (figure 7)

In the surrounding of the valve, the fluid vena geometry is rapidly modified by the disc angular position and, as for a flexible pipe, the wave velocity falls down : the reflected compression wave cannot reach the valve before its closure. In the same way, later in the transient, this flexible pipe behaviour damps the two effects when a wave impinges

the disc (figures 3,4 and 5).

### 2.2.3 Disc bounce effect (fig. 6, 7, 8, 9, 10)

In the last instants before closure, the section of the gap between the disc and its seat rapidly decreases. The fluid is quickened and the pressure tends to the local saturation pressure. If it is reached (temperature or no compression wave) the flow beneath the disc becomes choked. To close, the disc must flatten out the fluid vena. This causes a pressure increase that opposes the pressure drop.

This forces the disc to stop or to bounce according to the local fluid compressibility and condensation. If it bounces, the inversion of the induced flow rate generates down-stream a pressure surge.

In the third test, the flow is choked at 124ms (figure 9). Down-stream the pressure increases slightly from 125 to 136ms (figure 10). Then the final pressure surge occurs. Since no bounce pressure surge appears in figure 10, the disc in the third test stops when the flow is choked. The delay between the instant of bounce (58ms, figure 8) and the instant where the surge is in A (62ms, figure 7) backs up the assertion of a flexible pipe behaviour of the fluid vena. The total closure surge superimposes on this surge.

The experimental results are summarized in table 1.

## 3 - MODELLING OF THE DISC BEHAVIOUR

From the test analysis, a model of swing check valve has been developed to take the three first effects into account. The fourth effect is more difficult to model and is not presented here. No attempt was made to model the fluid vena behaviour in the surrounding of the valve. This model is implanted in the ATHIS code (2) which solves for complex piping systems and for water, vapour or two phase mixture the one dimensional equations of fluid motion by the method of characteristics. The model is illustrated by the sketch in figure 12.

### 3.1 Cross Section

The check valve is represented by a short pipe. Its cross section, the area left free by the valve disc in the pipe, is a function of  $\theta$ . This section, constant along the pipe, is obtained from drawings.

### 3.2 Induced flow rate and head loss

We suppose that the flow induced by the disc motion is accurately represented by :  $\dot{m} = \rho \pi R^2 d\theta$

Where  $\rho$  is the arithmetical mean of the local fluid density at each part of the junction :

$$\text{junction 1 : } \rho = (\rho_a + \rho_b)/2$$

$$\text{junction 2 : } \rho = (\rho_c + \rho_d)/2$$

At each end of the valve, the two characteristics, the continuity and the energy equations are solved with the following assumptions :

-The pipe flow rate is the sum of the flow rate through the contracted area of the valve and the induced flow rate :

$$\begin{aligned} \text{junction 1 : } \rho_a v_a A &= \rho_b v_b A_v + \dot{m} \\ \text{junction 2 : } \rho_d v_d A &= \rho_c v_c A_v + \dot{m} \end{aligned}$$

- The head loss is located at the up-stream end of the valve and calculated with the flow velocity beneath the valve door (3). This allows us to match the experimental determination of the head loss coefficient in reverse flow K (permanent flow).

A mesh point is used to join the ends of the valve by the mean of the usual equations.

### 3.3 Disc dynamics (figure 12)

If we assume that :

- the centre of pressure and the centre of gravity are identical during the motion,

- the hydrodynamic forces resultant on the disc can be approximate by  $S(P_a - P_d)$  where S is the part of the disc area actually fritting in the flow (figure 2) and determined from drawings, the disc movement equation can be written as :

$$I\ddot{\theta} = -Mg d \sin \theta + S(P_a - P_d)$$

I is the total inertia of the valve. It can be set as (4) :

$$I = I_o + I_{add}$$

$I_o$  is the disc inertia

$I_{add}$  is the added inertia which represents the inertia of the fluid dragged by the disc and depends on the fluid temperature and the length of the pipe representing the valve.

## 4 - COMPARISON BETWEEN TEST DATA AND CALCULATIONS

The model was run for three tests presented above. The figures 3 to 10 show the results of the calculations which are summarized in table 1. For the first test, the computed disc course and closure time agree very well with the data. In spite of a mismatch on the wave propagation and a little saturation of the pressure transducer PB, computed intensity and duration of the waterhammer are in good agreement with the measured results.

The absence of the fourth effect in the model and the lack of the fluid area flexible pipe behaviour modelisation is somewhat detrimental to a good match between calculations and experiments for the second and third tests:

The figures 6 to 8 show that the fluid-disc interaction assumed for the calculations is less strong than in the tests :

- waves generated by the initial disc acceleration exist in the calculations but they are less important than in the test and hardly visible on the figure 7.

- the initial expansion wave slope is not smoothed off by the disc motion and the reflected wave reaches the valve before closure. So the flow beneath the disc cannot be choked.

Nevertheless, outside the bounce zone, the disc course is well computed. It appears clearly that the wave effect is essential when the disc is at rest and that the head loss effect is the closing force when the disc moves.

Since the disc closes earlier in the calculations, the flow rate in the pipe is necessarily lower and the waterhammer less important. The gap between calculated and measured values is less than 10 % for the pressure surge.

In the third test, condensation occurs in PA at 118ms but the initial expansion wave is stronger in the experiment (figure 9). The valve closes at 125ms and the pressure surge reaches point B at 126ms. The calculated waterhammer is less than 10 % smaller than the actual one.

## 5 - CONCLUSION

The experiments carried out on the test facility CLAUDIA at CEA Cadarache (FRANCE) reveal four main effects during the closure of a swing check valve : the head loss effect, the wave effect, the induced flow rate effect and the bounce effect. A model has been developed to take the three first effects into account. The lack of the fourth effect, more difficult to compute, is obviously detrimental to a good agreement between the test data and the calculated results, but the mismatch remains reasonable ; the calculated waterhammer is less than 10 % smaller than the actual one. When the fourth effect does not affect the transient, the model is very near the actual behaviour of the valve disc and the waterhammer very well reproduced.

### SYMBOLS

A : pipe cross section	K : head loss coefficient
$A_v$ : valve contracted area	M : disc weight
d : distance between the axis of rotation and the centre of gravity	P : pressure
g : gravity acceleration	R : disc radius
I : total valve inertia	v : fluid velocity
	$\rho$ : fluid density
	$\theta$ : disc angle

### REFERENCES

- HUET, J.L., GARCIA, J.L., COPPOLANI, P. & ZIEGLER, B. 1987 - Experimental and analytical studies on waterhammer generated by the closing of check valves. This Conference - Division F
- MONHARDT, D. & ROUSSET, P. Programme de calcul ATHIS, Manuel d'utilisation. Rapport technique FRAMATOME FRATEC 211.
- PROVOOST, G.A. 1983. A critical analysis to determine dynamic characteristics of non-return valves. 4th Int. Conf. on Pressure Surges
- THORLEY, A.R.D. 1983. Dynamic response of check valves. 4th Int. Conf. on Pressure Surges.

Table 1

TEST	CLOSURE TIME (M S)		PRESSURE SURGE IN B (bar)	
	measured	computed	measured	computed
1	121	123	250	257
2	105;58*	57	155 - 160	144
3	-	125	175 - 180	162

\* first bounce

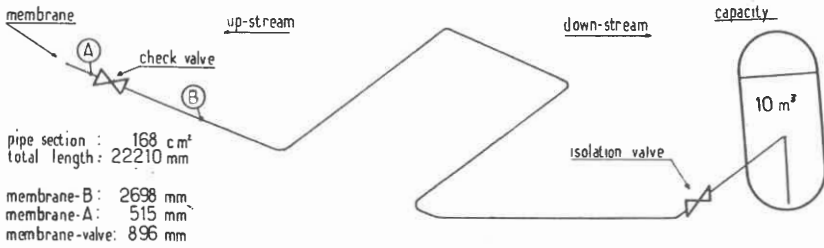


Figure 1

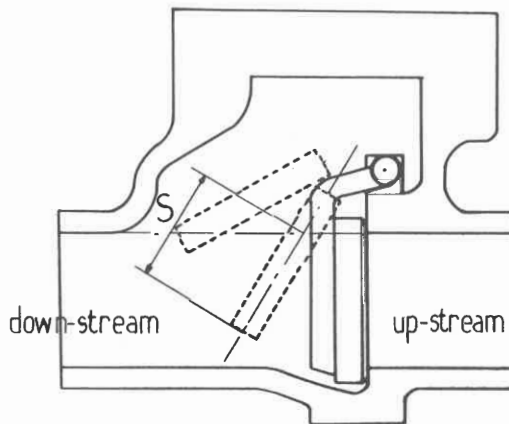


Figure 2

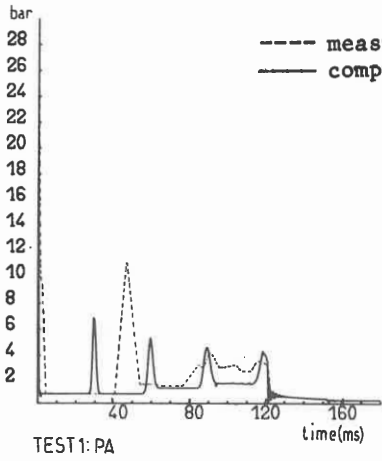


Figure 3

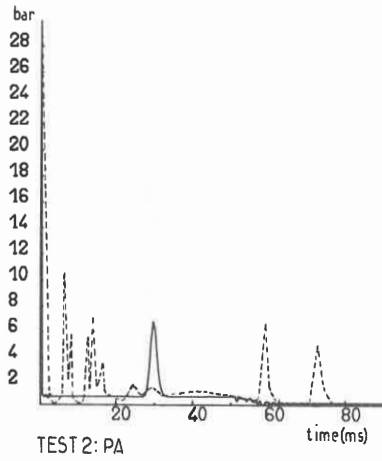


Figure 6

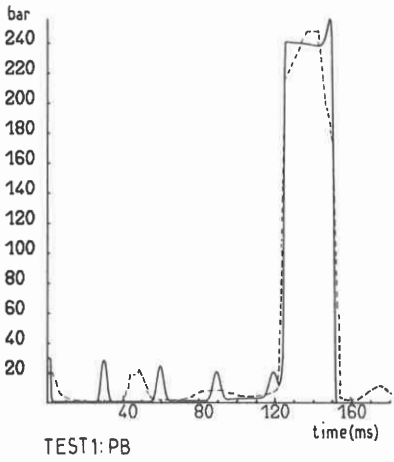


Figure 4

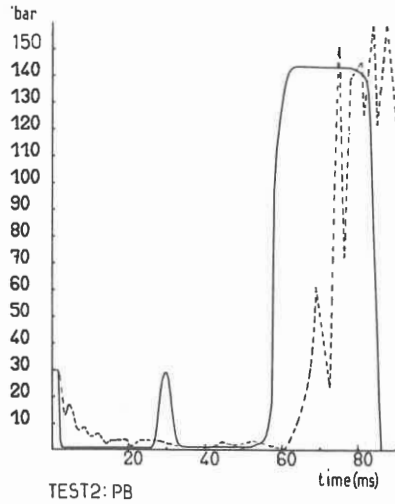


Figure 7

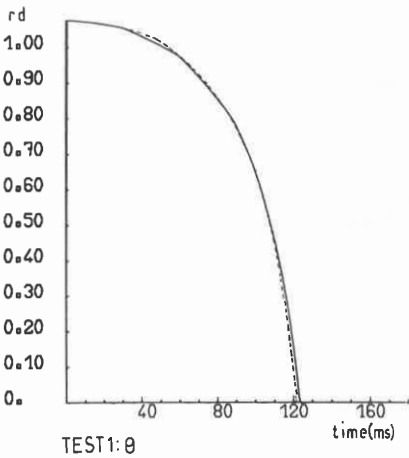


Figure 5

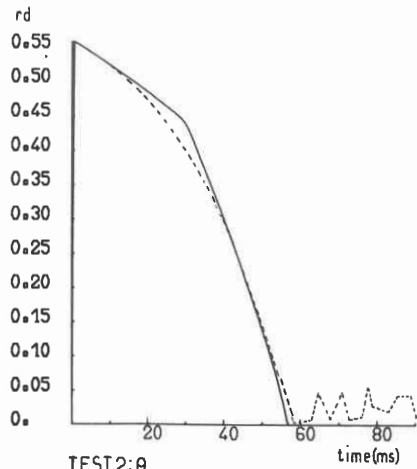


Figure 8

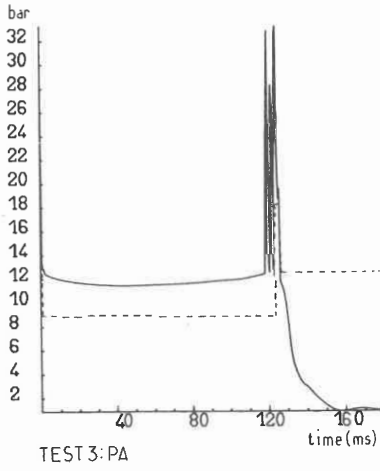


Figure 9

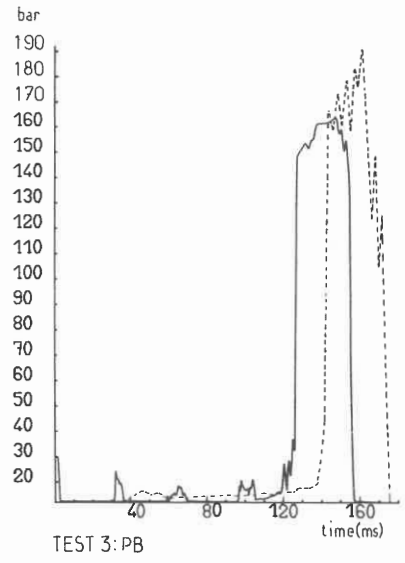


Figure 10

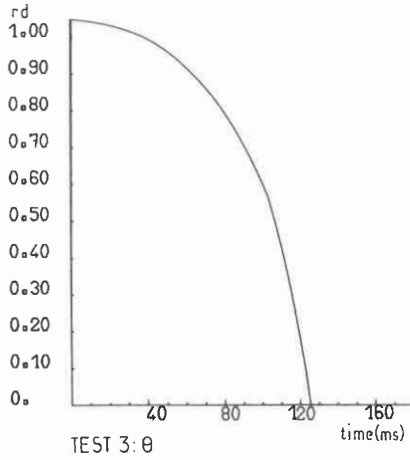


Figure 11

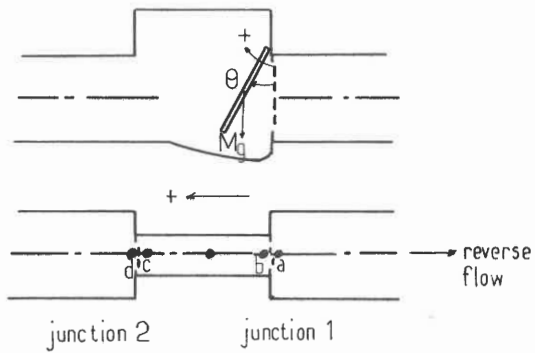


Figure 12